Pergamon

PII: S0301-9322(97)00013-X

CLASSIFICATION OF INSTABILITIES IN PARALLEL TWO-PHASE FLOW

P. A. M. BOOMKAMP[1,2] and R. H. M. MIESEN[1]

[1]Shell Research and Technology Centre, P.O. Box 38000, 1030 BN Amsterdam, The Netherlands
[2]University of Twente, P.O. Box 217, 7500 AE Enschede, The Netherlands

Abstract—There is extensive literature on the stability of parallel two-phase flow, both in the context of liquid–liquid as well as gas–liquid flow. Aimed at making this literature more transparent, this paper presents a classification scheme for the various instabilities arising in parallel two-phase flow. To achieve such a classification, the equation governing the rate of change of the kinetic energy of the disturbances is evaluated for relevant values of the physical parameters. This shows the existence of five different ways of energy transfer from the primary to the disturbed flow, which have their origin in density stratification, velocity profile curvature, viscosity stratification or shear effects. Each class is discussed on the basis of references covering the developments over the last 35 years. © 1997 Elsevier Science Ltd.

Key Words: stratified flow, two-phase flow, linear stability, gas–liquid flow, liquid–liquid flow, horizontal flow, vertical flow

1. INTRODUCTION

More than a century ago, the basic concepts of the linear theory of hydrodynamic stability were formulated by, among others, Kelvin, Reynolds, Taylor and Rayleigh. As the implications of this theory for single-phase, parallel, shear flow may be considered as well-documented since about 15 years (see, for instance, Drazin and Reid 1981), attention has shifted to the stability of two-phase flow. Apart from its clear academic relevance, this research is motivated by its technological importance, with applications in aviation (Yih 1990), coating technology (Wang 1978), and in the nuclear and petrochemical industry (Hall-Taylor and Hewitt 1962; Miesen and Boersma 1995).

Undoubtedly the most appealing example of unstable gas–liquid flow is the generation of water waves by wind. This phenomenon has received much attention through the years, both in the context of deep water and thin films. In the fifties and sixties important steps towards the understanding of wave-formation in air–water flow have been taken by Miles and Benjamin. Miles (1957, 1959a, 1959b, 1962, 1967) has written a series of papers, entitled "On the generation of surface waves by shear flow", discussing some of the physical mechanisms that may be responsible for the energy transfer to these waves. Building upon the first paper of Miles, Benjamin (1959) presented a 'quasi-static' approximation to tackle the air–water stability problem. This so-called 'divided attack' was, for instance, applied by Miles (1962) to the problem of the generation of waves on deep water and by Cohen and Hanratty (1965) and Craik (1966) for thin films.

In the last decade, emphasis in research on the stability of two-phase flow has gradually shifted towards liquid–liquid systems. A strong impulse in this direction has been given by the interest in core–annular flow, a technique used to facilitate the transport of viscous oil through a pipeline by lubricating it with a 'low-viscosity' liquid such as water (for details, see Joseph and Renardy 1993). Consequently, there have been numerous investigations into the stability of the interface of two shearing fluids with different viscosities. These studies are based on a pioneering analysis by Yih (1967), who showed that viscosity stratification can induce instability in plane Couette–Poiseuille flow.

The huge amount of literature on the stability of two-phase flow shows that this type of flow is susceptible to instabilities of various kinds. Besides instability caused by viscosity stratification,

mentioned above, instability can result from density stratification, velocity profile curvature or from shear effects in one of the constitutive phases. It is, however, hard to get an overview of this literature. This lack of transparency can be ascribed to the fact that, unlike for the single-phase stability problem where the Reynolds number is the only parameter, the formulation of the two-phase stability problem requires at least six dimensionless parameters. Due to this complexity, studies in this field usually apply to a relatively small region in parameter space, which implies that it is not always clear whether two arbitrary papers study the same *type* of instability or not. One should note that it is generally not possible to give direct and simple explanations of these instabilities. The physical arguments given by Lighthill (1962), Hinch (1964) and Smith (1990) are valid under *specific* conditions only.

In the light of the above, a scheme in which the various instabilities in parallel two-phase flow can be classified would make the literature more transparent. In this paper, we present a classification scheme that covers the developments over the last 35 years, while containing as few classes as possible. In an attempt to obtain some insight into the nature of the different instabilities, we investigate the way of energy transfer from the primary to the disturbed flow (Hooper and Boyd 1983; Hu and Joseph 1989). Such an energy analysis is based on the fact that, by definition, instability implies the increase of kinetic energy of an initially small disturbance with time. In two-phase flow, mechanisms of different physical origin account for the production of this energy. Identification of the dominant mechanism of energy production then allows us to discriminate between different types of waves. The first to derive the energy equation for parallel two-phase flow were Hooper and Boyd (1983). Subsequently, Hu and Joseph (1989) used the same method to compute the various energy terms for the disturbances with the maximum growth rates. Referring to the successful experiences with energy considerations of this kind by Hooper and Boyd (1983, 1987), Hu and Joseph (1989), Kelly *et al.* (1989), Chen *et al.* (1990), Bai *et al.* (1992), Dijkstra (1992) and Joseph and Renardy (1993), we may expect the above procedure to provide enough information to point out the physical characteristics of the various instabilities in two-phase flow.

This paper is organized as follows. In section 2, the two-phase stability problem is formulate⁻¹ and attention is subsequently focused on the equation governing the average rate of change of disturbance kinetic energy. In order to achieve a classification of the various instabilities, this equation is evaluated numerically for characteristic combinations of the physical parameters (section 3). Our computations show that five classes of instability can be distinguished; in each subsection, a separate class is discussed on the basis of references.

2. THEORETICAL FRAMEWORK

2.1. Formulation of the stability problem

Because the purpose of this paper is to give an overview of the instabilities in two-phase flow, the formulation of the stability problem must allow for widely divergent flow systems like, for instance, wind over the surface of the ocean, liquid–liquid flow in a channel and film flow down an inclined plane. To ascertain generality, the specification of the primary flow will therefore be delayed until a fairly advanced stage in the analysis.

The flow configuration is shown schematically in figure 1. The two fluids, labeled $j = 1, 2$, are
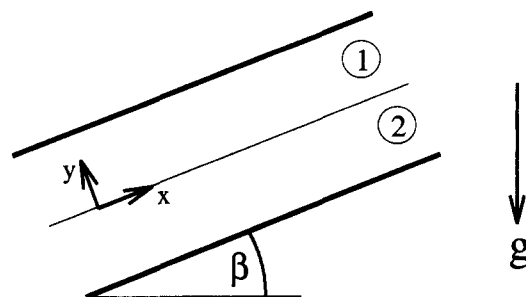

Figure 1. The flow configuration.

immiscible and incompressible. Dynamic viscosity, density and layer thickness are denoted by μ_j, ρ_j and d_j, respectively; the angle of inclination from the horizontal is β and $\mathbf{g}$ is the gravitational acceleration. The coordinates along and perpendicular to the undisturbed interface are x and y, respectively, with the origin of y chosen at the interface. Unbounded flow is described by considering it as a limiting case of bounded flow, i.e. by taking a very large value of the layer thickness of the fluid in question. In the following it will be convenient to use dimensionless quantities. Using the same conventions as Miesen and Boersma (1995), we write variables in dimensionless form by scaling length with the thickness of the lower layer d_2, velocity with a characteristic velocity U_i, time with d_2/U_i and pressure with $\rho_2 U_i^2$. The characteristic velocity U_i is defined as $U_i = \tau d_2/u_2$, where τ is the shear stress at the interface; this velocity is equal to the interfacial speed if the basic-state velocity profile $U_2(y)$ is linear.

By assumption, the primary flow is a solution of the time-independent Navier–Stokes equations, driven by a pressure gradient, by a shear stress or by gravity. When the flow in both phases is laminar, the velocity profiles $U_j(y)$ can be calculated exactly. However, when the flow in one of the two phases is turbulent, we will use a 'quasi-steady' description of the flow in that phase, i.e. we then assume the velocity profile to be given by its time-averaged value. This approach seems justified in view of, for instance, the recent work of Kuru et al. (1995), who present growth rate calculations for both laminar as well as turbulent air flow over water, finding only small differences if the friction velocity and the liquid height are taken the same. We note that their conclusion that the primary effect of turbulence is through changes in the time-averaged velocity profile is also supported by observation: liquid films can have a perfectly smooth surface in the presence of a turbulent gas flow if the mean air velocity is below a certain critical value (Cohen and Hanratty 1965). In fact, this suggests that the time scale corresponding to the turbulent fluctuations is in general much shorter than that of the growth of disturbances of the time-averaged flow (typically 10^{-6} s (Schlichting 1955) vs 10^{-2} s (Miesen and Boersma 1995) for wind over water). For air–water flow, the role of turbulence is extensively discussed by Miles (1959c, 1967, 1993) and Van Duin and Janssen (1992).

The stability of the flow configuration in figure 1 is investigated by disturbing the primary flow infinitesimally (Drazin and Reid 1981). Therefore, the velocity components and the pressure are written as a time-independent component (the primary flow) plus a time-dependent disturbance. We can restrict ourselves to an analysis of the behaviour of two-dimensional disturbances, because it was shown by Squire (1933) and Yih (1955) that by means of a simple transformation the stability for three-dimensional disturbances can be related to the stability for two-dimensional disturbances, the latter always being more unstable.

Using the presumptions that the flow is two-dimensional and incompressible, we represent the disturbance velocities in the fluids by the streamfunctions $\Psi_j(x, y, t)$. Because the primary flow $U_j(y)$ only depends on the y-coordinate, we assume the streamfunctions to have the form (Drazin and Reid 1981)

$$\Psi_j(x, y, t) = \psi_j(y)\, e^{i\alpha(x - ct)}, \tag{1}$$

where i is the imaginary unit. We concentrate on the temporal growth of the disturbances by taking α as a (prescribed and) real wavenumber, and allowing the wave speed c to be complex. The real part of c gives the phase velocity of the wave, while the imaginary part of αc is the growth rate (positive if $\text{Im}(\alpha c) > 0$).

Substitution of the streamfunctions $\Psi_j(x, y, t)$ into the linearized Navier–Stokes equations results in the well-known Orr–Sommerfeld equations for the y-dependent functions $\psi_j(y)$. Writing these equations in dimensionless form gives (Yiantsios and Higgins 1988)

$$\psi_1'''' - 2\alpha^2 \psi_1'' + \alpha^4 \psi_1 = (i\alpha Rr/m)[(U_1 - c)(\psi_1'' - \alpha^2 \psi_1) - U_1'' \psi_1], \tag{2}$$

for the upper phase $(0 < y < n)$, and

$$\psi_2'''' - 2\alpha^2 \psi_2'' + \alpha^4 \psi_2 = i\alpha R[(U_2 - c)(\psi_2'' - \alpha^2 \psi_2) - U_2'' \psi_2], \tag{3}$$

for the lower phase $(-1 < y < 0)$. Primes are used to indicate differentiation with respect to y, the Reynolds number is defined as $R = \rho_2 U_i d_2/\mu_2$, and the ratios r, m and n are defined as $r = \rho_1/\rho_2$, $m = \mu_1/\mu_2$, $n = d_1/d_2$.

The boundary conditions expressing no-slip and no-penetration at the rigid channel walls are

$$\psi_1 = \psi_1' = 0, \text{ at } y = n, \tag{4}$$

$$\psi_2 = \psi_2' = 0, \text{ at } y = -1. \tag{5}$$

The conditions at the interface are the continuity of the velocity components and the balance of the stress components. Formally speaking, these conditions must be evaluated at $y = \eta(x, t)$, the location of the interface in the disturbed flow, and not at the originally flat interface $y = 0$. This modification is taken into account by means of a Taylor expansion in η around $y = 0$. Correct to the leading order in η, the interface conditions then read (Yih 1967; Miesen and Boersma 1995)

$$\psi_1 = \psi_2, \text{ at } y = 0, \tag{6}$$

$$\psi_1' + U_1'\psi_1/c = \psi_2' + U_2'\psi_2/c, \text{ at } y = 0, \tag{7}$$

$$m(\psi_1'' + \alpha^2\psi_1 + U_1''\psi_1/c) = \psi_2'' + \alpha^2\psi_2 + U_2''\psi_2/c, \text{ at } y = 0, \tag{8}$$

$$m(\psi_1''' - 3\alpha^2\psi_1') + i\alpha R(c\psi_1' + U_1'\psi_1) - (\psi_2''' - 3\alpha^2\psi_2') - i\alpha R(c\psi_2' + U_2'\psi_2)$$
$$+ i\alpha R(F\cos\beta + \alpha^2 S)\psi_2/c = 0, \text{ at } y = 0, \tag{9}$$

where $S = \sigma/(\rho_2 U_i^2 d_2)$ is an inverse Weber number based on the interfacial tension σ, and $F = g(\rho_2 - \rho_1)d_2/(\rho_2 U_i^2)$ is an inverse Froude number. In deriving the interface conditions [6]–[9], we have used that the shear stress in the primary flow is continuous across the interface: $U_2' = mU_1'$ at $y = 0$. Moreover, we have introduced the convention that the reference frame moves with the interfacial speed, i.e. $U_1 = U_2 = 0$ at $y = 0$.

The flow equations [2]–[3] and the boundary and interface conditions [4]–[9] constitute an eigenvalue problem for the complex wave speed c. In order that the solution of this homogeneous differential system is not identical to zero, the wave speed c must take on specific values. Modern computational facilities allow us to solve this eigenvalue problem entirely numerically for almost any prescribed primary profile $U_j(y)$ and a large range of the dimensionless parameters α, R, m, r, n, S, F and β. Following the method described in the papers by Miesen and Boersma (1995) and Boomkamp et al. (1997) we solve the problem by means of a spectral technique, based on an expansion of the functions $\psi_j(y)$ in Chebyshev polynomials and on point collocation. Subsequent solution of the resulting generalized eigenvalue problem with the QZ-algorithm (Molar and Stewart 1973; NAG 1988) then provides the dispersion relation

$$c = c(\alpha, R, m, r, n, S, F, \beta), \tag{10}$$

and the corresponding eigenfunctions $\psi_j(y)$. These eigenfunctions determine the stream functions $\Psi_j(x, y, t)$, as defined as [1], which contain all information about the velocity and pressure disturbances in the linear stability problem. By comparing numerical results with the asymptotic results of Craik (1966), Van Gastel et al. (1985) and Yih (1990), Miesen and Boersma (1995) have in fact already shown that the computer code for the numerical solution of the problem works well. We have nevertheless checked the correctness of the code once again by reproducing the asymptotic results of Yih (1967) and Hooper and Boyd (1983) as well as the numerical results of Yiantsios and Higgins (1988) and Hooper (1989).

2.2. Energy balance

A flow being unstable implies that the kinetic energy of initially small disturbances grows with time. Although it is evident that this energy is always being supplied by the primary flow, it is in general not clear by which mechanism this takes place. In two-phase flow, it is for example possible that an instability receives its energy from the flow in the bulk of either of the two phases, similar to the mechanisms in single-phase flow. It may also occur that an instability originates at the interface, or that the energy originates from more than one source. A way to understand these different mechanisms of energy transfer is to consider equation [52] of Hooper and Boyd (1983) or [5.2] of Hu and Joseph (1989), equations which describe how the rate of change of the

disturbance kinetic energy is composed of energy production and dissipation terms. For the sake of clarity, we will include a concise derivation of this equation.

The Navier–Stokes equations express conservation of mass and momentum of a fluid. Multiplying the momentum equation with a velocity gives an expression in which terms can be interpreted as some kind of energy. We therefore take the inner product of the velocity disturbances (u_j, v_j) with these equations. Subsequently, we average over a wavelength $\lambda = 2\pi/\alpha$ and integrate over the thickness of the fluid. Doing this for both the upper and the lower fluid, adding the two results and applying the divergence theorem of Gauss, we obtain the equation

$$\sum_{j=1}^{2} KIN_j = \sum_{j=1}^{2} DIS_j + \sum_{j=1}^{2} REY_j + INT. \tag{11}$$

Here, the volume contribution of each fluid to the energy balance is decomposed into three terms:

$$KIN_j = \frac{r_j}{\lambda} \frac{d}{dt} \int_{a_j}^{b_j} dy \int_0^{\lambda} dx \left[\frac{1}{2} (u_j^2 + v_j^2) \right], \tag{12}$$

$$DIS_j = -\frac{m_j}{\lambda R} \int_{a_j}^{b_j} dy \int_0^{\lambda} dx [2(u_{j,x})^2 + (u_{j,y} + v_{j,x})^2 + 2(v_j,y)^2], \tag{13}$$

$$REY_j = \frac{r_j}{\lambda} \int_{a_j}^{b_j} dy \int_0^{\lambda} dx \left[(-u_j v_j) \frac{dU_j}{dy} \right], \tag{14}$$

with $j = 1$, $m_1 = m$, $r_1 = r$, $a_1 = 0$, $b_1 = n$ for the upper fluid and $j = 2$, $m_2 = 1$, $r_2 = 1$, $a_2 = -1$, $b_2 = 0$ for the lower fluid. Subscripts x and y indicate partial differentiation. Characteristic for a multiphase system is the presence of an energy contribution INT that is associated with the existence of an interface (Hu and Joseph 1989). It is convenient to decompose this contribution into

$$INT = NOR + TAN, \tag{15}$$

where

$$NOR = \frac{1}{\lambda} \int_0^{\lambda} dx [v_2 T_2^{(yy)} - v_1 T_1^{(yy)}]_{y=0}, \tag{16}$$

$$TAN = \frac{1}{\lambda} \int_0^{\lambda} dx [u_2 T_2^{(xy)} - u_1 T_1^{(xy)}]_{y=0}, \tag{17}$$

and we have introduced the components $T_j^{(xy)}$ and $T_j^{(yy)}$ of the stress tensor of the disturbed flow

$$T_j^{(xy)} = \frac{m_j}{R} (u_{j,y} + v_{j,x}), \quad T_j^{(yy)} = -p_j + 2\frac{m_j}{R} v_{j,y}, \tag{18}$$

where p_j denote the pressure disturbances.

Our discussion on the physical meaning of the different terms in the energy equation [11] summarizes the clear one given by Kelly et al. (1989). The terms KIN_j represent the spatially averaged rate of change of the disturbance kinetic energy. For an unstable flow, the kinetic energy of initially small disturbances grows with time, and the rates of change [12] are both positive (the time derivative d/dt in [12] corresponds to multiplying with $Im(2\alpha c)$, which has the same value in both fluids). The terms DIS_j represent the rate of viscous dissipation of the disturbed flow in each fluid. As expected, viscous dissipation opposes instability, which can be seen from the minus sign in [13]. Since the Reynolds stress $\tau_j(y)$ in the disturbed flow is given by (Lin 1955)

$$\tau_j(y) = -\frac{r_j}{\lambda} \int_0^{\lambda} \mathrm{d}x[u_j v_j], \tag{19}$$

the terms REY_j represent the rate at which the Reynolds stress is transferring energy between the primary flow and the disturbed flow. The terms [14] can either stabilize or destabilize the primary flow, depending on the details of the problem.

The energy contribution INT represents the rate of work done in deforming the interface. The rate at which work is done by the velocity and stress disturbances in the direction normal to the interface is denoted by NOR, while TAN gives this rate for the disturbances in the tangential direction, i.e. in the direction of the primary flow. Insight into the physical meaning of NOR may be obtained by using the interface conditions [6] and [9]. After writing these conditions in terms of the normal velocity and stress disturbances (Miesen 1993), combining [6], [9], [16] and [18], and using the fact that the pressure in the primary flow satisfies $P_{1,y} - P_{2,y} = F \cos \beta$, the interface contribution NOR can be written as

$$NOR = \frac{1}{\lambda} \int_0^{\lambda} \mathrm{d}x[v S \eta_{xx}]_{u=0} + \frac{1}{\lambda} \int_0^{\lambda} \mathrm{d}x[v F \cos \beta \eta]_{y=0}, \tag{20}$$

where we have defined $v := (v_1 = v_2$ at $y = 0$. The first term represents the rate of work done against the interfacial tension in deforming the interface. In the unstable regime, the interface area increases and energy is stored in the disturbed flow in order to overcome the restoring effect of interfacial tension. In the stable regime, however, energy is being released. Similarly, the second term in [20] represents the rate of work done against the hydrostatic pressure gradient in deforming the interface. The interfacial tension energy contribution will be denoted by TEN and the hydrostatic contribution by HYD.

The interface term TAN, as defined in [17], represents the rate at which the tangential velocity and stress disturbances do work at the interface, and finds its origin in a jump in viscosity and/or density at the interface (Smith 1989, 1990). These two possibilities can readily be illustrated by studying the flow of two fluids of equal density, but different viscosity ($r = 1, m \neq 1$) and the flow of two fluids of equal viscosity, but different density ($m = 1, r \neq 1$). In both cases, it is instructive to write the interface conditions [7] and [8] in the form (Miesen 1993)

$$u_1 + \eta U_1' = u_2 + \eta_2', \text{ at } y = 0, \tag{21}$$

$$RT_1^{(xy)} + m\eta U_1'' = RT_2^{(xy)} + \eta U_2'', \text{ at } y = 0, \tag{22}$$

expressing continuity of tangential velocity and stress, respectively.

First, we isolate the effect of a jump in viscosity at the interface. For two fluids of equal density, conservation of momentum in the x-direction implies

$$mU_1'' = U_2'', \text{ at } y = 0, \tag{23}$$

as follows directly from the Navier–Stokes equations for the primary flow (Miesen 1993). Consequently, the disturbance shear stresses $T_j^{(xy)}$ are continuous across the interface (cf. [22]), which allows the energy term [17] to be written as

$$TAN_r := TAN = \frac{1}{\lambda} \int_0^{\lambda} \mathrm{d}x[(u_2 - u_1)T^{(xy)}]_{y=0} \text{ if } r = 1, \text{ or } \beta = 0, \tag{24}$$

where we have defined $T^{(xy)} := T_1^{(xy)} = T_2^{(xy)}$ at $y = 0$. Since the interface is not able to take up shear stress, the primary flow satisfies

$$mU_1' = U_2', \text{ at } y = 0, \tag{25}$$

creating a jump in the *slope* U_j' of the basic-state velocity profile. This means that when the interface is being deformed, velocity disturbances u_j are forced onto the interface to compensate for the gap in the velocity of the primary flow, as can be seen from [21]. Due to the jump in slope, however,

these disturbance velocities are discontinuous across the interface, i.e. $u_2 \neq u_1$, which involves a net† energy transfer [24] from the primary flow to the disturbed flow. Energy transfer of this kind may therefore be considered as "velocity-induced", as Smith (1990) calls it. Based on the central role played by viscosity in creating the jump in slope, Hu and Joseph (1989) use the term "interfacial friction". In the present paper, we will call the energy transfer [24] "viscosity-induced", indicated by TAN_r.

Next, we address the effect of a jump in density at the interface. If the densities differ and the angle of inclination β is nonzero, the equations of motion for the primary flow imply that the equality [23] is not valid anymore, i.e., the effect of gravity causes a jump in the *curvature* U_j'' on the basic-state velocity profile at the interface (Smith 1989, 1990). Obviously, in order to satisfy continuity of total shear stress [22], disturbance shear stresses $T_j^{(xy)}$ have to develop on both sides of the deformed interface. Due to the jump in curvature, however, these disturbance shear stresses are discontinuous across the interface, i.e. $T_2^{(xy)} \neq T_1^{(xy)}$, which for two fluids of equal viscosity involves a net energy transfer

$$TAN_g := TAN = \frac{1}{\lambda} \int_0^\lambda dx [u(T_2^{(xy)} - T_1^{(xy)})]|_{y=0} \text{ if } m = 1,$$ [26]

from the primary flow to the disturbed flow. In deriving [26], we have used [17], [22] and [25], and defined $u := u_1 = u_2$ at $y = 0$. Chen *et al.* (1990) emphasize the importance of gravity in creating the discontinuity in the disturbance shear stresses by indicating [26] as "interfacial gravity". In Smith's (1990) terminology, the interface energy TAN is now "stress-induced". We prefer to call the energy transfer [26] "gravity-induced", denoted by TAN_g.

We finally note that although we are dealing with a linear theory of hydrodynamic stability, the energy equation [11] is *second* order in η, the disturbance of the interface. Therefore, we may wonder if products of quantities that are of zeroth and second order in η, respectively, do contribute to the leading order energy equation. Contributions of this kind are however lost through averaging over one wavelength, so that [11] is indeed correct in studying the energy transfer to the disturbed flow.

3. CLASSIFICATION

The streamfunctions $\Psi_j(x, y, t)$ contain all information needed to calculate the velocity, the pressure and the interface disturbances (Miesen 1993). These functions are found by means of a Chebyshev collocation method (section 2.1). Hence, for each set of physical parameters, computation of the various terms that arise in the energy equation [11] can be performed in a straightforward manner. Recalling that six or more parameters are involved in the formulation of the problem, it is however important to ascertain that the way in which we scan the parameter space, physically makes sense. For a given gas–liquid or liquid–liquid combination, only the flow rates of the fluids can be varied experimentally; all other physical quantities are fixed. We therefore first choose the two fluids and specify the basic-state velocity profile $U_j(y)$. Subsequent computation of the energy terms KIN_j, DIS_j, REY_j, TEN, HYD and TAN for some typical values of the two flow rates then reveals the instabilities this specific flow system is susceptible to. The wavenumber is chosen to correspond to the most unstable one (Hu and Joseph 1989), so that a certain number of examples discussed below can also be found in the monograph of Joseph and Renardy (1993). Doing the above procedure for a sufficiently large number of fluid combinations provides an overview of the different kinds of instabilities in two-phase flow.

Before actually presenting this overview, we note that the numerical results of the abovementioned computations allow for an additional check on the consistency of the collocation method outlined in section 2.1. A natural estimate of the relative accuracy of the method is obtained

---

†Note that it <u>is also</u> possible to further decompose the interface contribution [17] into two separate terms $TAN_1 = -\overline{u_1 T_1^{(xy)}}$ and $TAN_2 = \overline{u_2 T_2^{(xy)}}$, where the bar denotes averaging over one wavelength. Such a refinement may provide additional information about the role of either of the two phases in the energy transfer at the interface. We shall return to this point in section 4.

Table 1. Energy distribution for the Rayleigh–Taylor instability, which receives its energy from the work done by the normal component of gravity at the interface, HYD. The energy terms are for plane oil–water Couette flow in a channel with $\alpha = 1.80$, $R = 1.44 \times 10^{-3}$, $m = 0.05$, $r = 1.16$, $n = 0.1$, $S = 2.08 \times 10^8$, $F = -1.39 \times 10^9$, $\beta = 0$. The physical properties of the oil and the water have been taken from Kao and Park (1972)

KIN_1	KIN_2	DIS_1	DIS_2	REY_1	REY_2	TEN	HYD	TAN_i
0.74	0.26	−3.31	−0.76	0.00	−0.00	−4.80	**9.87**	0.00

by comparing the residual of [11]—as calculated by adding all energy terms—to the term with the largest absolute value. For the parameter values used in table 1, this implies for instance a relative error of the order 10^{-7}; for the other tables presented in this paper, the error is of the order 10^{-5} or less.

Our numerical computations show that if instabilities driven by the same energy term(s) are grouped together, five classes of instability can be distinguished. In each subsection below, a separate class is discussed.

3.1. Rayleigh–Taylor instability

A two-fluid system composed of a heavy fluid overlying a light one will develop instability, because for sufficiently long waves the destabilizing gravity forces are larger than the restoring forces resulting from interfacial tension. This kind of instability is called Rayleigh–Taylor instability after the pioneering work by Rayleigh (1883) and Taylor (1950), and applies both to two fluids in rest as well as low velocity. As indicated by Taylor, the same kind of instability will arise if the gravitational acceleration is replaced by any other acceleration.

Table 1 gives an account of the magnitude of the energy contributions for Rayleigh–Taylor instability in plane oil–water Couette flow with a low Reynolds number. Because of the arbitrary normalization of the streamfunction in linear theory, only the relative values of these contributions can be ascribed physical meaning to. We have scaled the terms by the total rate of change of kinetic energy, so that $KIN_1 + KIN_2 = 1$. This means that only energy terms of $\mathcal{O}(1)$ or larger significantly affect the instability.

Evidently, the Rayleigh–Taylor instability receives its energy from the work done by the normal component of gravity at the interface, HYD. The major part of this energy is used to overcome the restoring effect of interfacial tension and dissipation; the remainder is converted into kinetic energy. Theoretical and experimental progress on this type of instability has been made by Lewis (1950), Chandrasekhar (1961), Plesset and Whipple (1974), Whitehead and Luther (1975), Craik (1976), Prosperetti (1981), Yiantsios and Higgins (1989), and many others. A comprehensive list of references can be found in a review paper by Whitehead (1988).

3.2. Miles-instability

Some 35 years ago, Miles wrote a celebrated series of papers on the generation of surface waves by shear flows. In the first two parts of this series (Miles 1957, 1959a), he proposes an inviscid mechanism for the energy transfer from wind to waves on deep water, thus providing an explanation for the so-called "sheltering coefficient" introduced by Jeffreys (1925) 30 years before. A key role in Miles' asymptotic theory is played by the critical layer $y = y_c$, the layer where the wave speed equals the mean wind speed. Since the air flow is turbulent, the velocity profile $U_1(y)$ is characterized by a viscous sublayer adjacent to the water surface, where the velocity profile is linear, and a turbulent region above this layer with negative profile curvature. Provided that the wind speed is not too large, the critical layer is located outside the viscous sublayer for waves that are sufficiently long. Assuming inviscid flow in the air, Miles showed that the negative velocity profile curvature in the critical layer then induces a positive and constant Reynolds stress at all heights up to the critical $(0 < y \leqslant y_c)$. This wave-induced Reynolds stress, which should not be confused with the usual turbulence Reynolds stress, has a destabilizing effect and transfers energy (cf. [14]) to gravity waves with a wavelength of typically 10 cm. Note that if the critical layer is located inside the viscous sublayer, where the velocity profile curvature is identically zero, the Miles-mechanism cannot play a role in wave generation.

Table 2. Energy distribution for the Miles-instability, which receives its energy from the Reynolds stress in the air, REY_1. Parameter values correspond to wind over deep water, using a linear–logarithmic profile in the air [27] and an exponential profile in the water [28]. The parameter values used are $s = 5$, $n = \infty$, $b = 0.8$, $\alpha = 40$, $R = 7.5 \times 10^5$, $m = 0.018$, $r = 0.0012$, $S = 6.58 \times 10^{-5}$, $F = 2.18$, $\beta = 0$. This corresponds to (in SI-units) $g = 9.8$, $\sigma = 0.074$, $\rho_1 = 1.2$, $\rho_2 = 1000$, $\mu_1 = 1.8 \times 10^{-5}$, $\mu_2 = 0.001$, $d_2 = 0.5$, $u_* = 0.05$, $\tau = \rho_1 u_*^2 = 0.003$, $U_0 = 0.03$, $U_i = 1.5$, $\lambda = 7.86 \times 10^{-2}$. The corresponding Reynolds stress distribution is shown in figure 2

KIN_1	KIN_2	DIS_1	DIS_2	REY_1	REY_2	TEN	HYD	TAN_r
0.01	0.99	-6.10	-4.26	**12.86**	-0.24	-0.05	-1.01	-0.21

In order to check Miles' view on the formation of gravity waves numerically, we approximate the (dimensional) time-averaged wind profile by (Miles 1962)

$$U_1(y) = (\tau/\mu_1)y, \quad 0 \leqslant y \leqslant s\mu_1\sqrt{\rho_1\tau},$$

$$U_1(y) = \sqrt{\tau/\rho_1}[s + (\gamma - \tanh\tfrac{1}{2}\gamma)/\kappa], \quad y \geqslant s\mu_1/\sqrt{\rho_1\tau},$$

$$\sinh\gamma = \frac{2\kappa\sqrt{\rho_1\tau}}{\mu_1}[y - s\mu_1/\sqrt{\rho_1\tau}], \qquad [27]$$

corresponding to smooth flow over open water. Here, τ is the shear stress that the air exerts on the water surface, $\kappa = 0.4$ is the Von Kármán constant and s determines the thickness of the viscous sublayer (taken to be between 5 and 8). The wind induces a current in the water, which can be approximated by, for instance, an exponential profile

$$U_2(y) = (U_0/U_i)[e^{(U_i y/U_0)} - 1], \qquad [28]$$

where U_0 is the interfacial speed, having a value of typically 60% of the friction velocity $u_* = \sqrt{\tau/\rho_1}$ (Van Gastel et al. 1985).

For low air velocities (u_* typically 0.05 m/s), numerical computations based on the velocity profiles [27]–[28] indeed retrieve a mode of instability that exhibits the above-mentioned characteristics of the Miles-instability, which thus bears out the significance of Miles' theory. The energy distribution for the Miles-instability is shown† in table 2 for a friction velocity $u_* = 0.05$ m/s, which corresponds to a wind speed of roughly 1.5 m/s at two meters above the water. The wavelength is about 8 cm. It is seen that the instability receives its energy from the Reynolds stress energy contribution in the air, REY_1. The Reynolds stress distribution $\tau_j(y)$ that is responsible for this energy transfer is indicated in figure 2. Note that even though the critical layer lies outside the viscous sublayer, there is no discontinuity in the Reynolds stress at the critical layer, i.e. the stress distribution is smooth. Remembering that Miles' original model (1957) does not account for viscous effects, it is clear that such a smooth distribution results from solving the viscous Orr–Sommerfeld equation [2] instead of its inviscid counterpart, the Rayleigh equation. (Strictly speaking, it might be argued that the inviscid Reynolds stress is discontinuous for neutral disturbances ($\text{Im}(c) = 0$) only (Lin 1955). Our computations show, however, that the Reynolds stress distribution is qualitatively the same for neutral and unstable disturbances. This implies that the smooth distribution in figure 2 is primarily due to viscous effects, not to the absence of neutral stability.)

Through the years, several authors have worked on the air–water stability problem posed by Miles. Interesting in view of the present classification scheme is especially the contribution of Lighthill (1962), who gives a theoretical interpretation of the Miles-instability in terms of the physical processes operating in the region of the critical layer (see also Belcher and Hunt 1993). The explanation in terms of energy transfer given above can be considered complementary to Lighthill's interpretation. Conte and Miles (1959) present a numerical method to solve the specific

†For unbounded flow over deep water, the energy contributions can be calculated as follows. To avoid numerical problems in the limit of large y-values, it is first assumed that the air velocity [27] remains constant above a certain height $y = b$. This allows for an analytical solution of the Orr–Sommerfeld equation in the region $y > b$ (Miesen and Boersma 1995). Next, the thickness of the water layer d_2 is chosen a few times the wavelength λ and the corresponding growth rate is calculated. Finally, the parameters b and d_2 are varied in such a way that the (dimensional) growth rate becomes independent of these parameters. The energy equation [11] is then evaluated for the wavelength at which the growth rate attains its maximum.
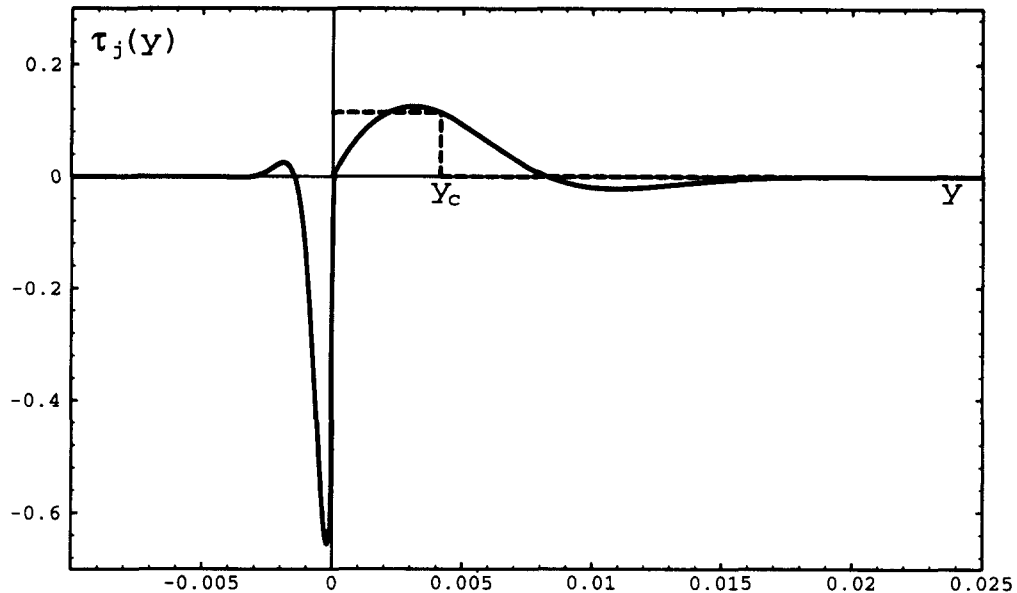
Figure 2. Characteristic Reynolds stress distribution $\tau_j(y)$ in the air ($j = 1, y > 0$) and in the water ($j = 2, y < 0$) for the Miles-instability (solid line). The parameter values used are the same as those in table 2. The Miles-instability is caused by the positive Reynolds stress in the air, which accounts for the energy production term REY_1 in table 2 (see [14]). The viscous sublayer adjoining the water surface reaches from $y = 0$ to 0.003, while the critical layer is located at $y_c = 0.0042$, i.e. *outside* the viscous sublayer. It is interesting to note that if the air had been assumed to be inviscid, the Reynolds stress would have been discontinuous at $y = y_c$ (Miles 1957) (dashed line). The vertical scale is arbitrary; outside the indicated interval the Reynolds stress is approximately zero.

boundary-value problem posed by Miles, while Morland and Saffman (1993) and Caponi *et al.* (1992) investigate the influence of distinct types of air and water velocity profiles on the growth rate of gravity waves. A concise review of field work performed to examine the validity of the Miles-mechanism can be found in Morland and Saffman (1993). The most extensive field study is probably that of Snyder *et al.* (1981): they measure pressure fluctuations above surface gravity waves and compare results with Long's (1980) model for the vertical structure of the pressure field, this model being derived from Miles's theory. Finally, we note that the Miles-instability corresponds to the "class-B instability" in Benjamin's well-known threefold classification of instabilities of the flow of a liquid over a flexible solid (Benjamin 1960, 1963; Kumaran 1995). Benjamin's other two classes of instability will be addressed in the sections 3.4 and 4.

3.3. Instability induced by tangential disturbances

The "instability induced by tangential disturbances" originates at the interface and is driven by the energy term TAN, which represents the rate at which work is done by the velocity and stress disturbances in the direction of the primary flow. In section 2.2, we have seen that this energy term can be considered "viscosity-induced" for horizontal flow ($\beta = 0$) or for two fluids of equal density ($r = 1$), and "gravity-induced" for two fluids of equal viscosity ($m = 1$). For these specific cases, the energy term TAN can be written as TAN_v and TAN_g, respectively (cf. [24] and [26]). In the *general* case of two fluids with different viscosities and densities, however, the effect of the viscosity jump and the effect of the density jump are coupled, i.e. it is then not possible to speak of either viscosity-induced or gravity-induced instability.[†] Because the origin of the energy term TAN can

---

†We may wonder whether it is possible to decompose TAN into a term that is proportional to the jump in viscosity, a term that is proportional to the jump in density, and a cross-term. Combination of [17], [21] and [22] shows that the magnitude of these three terms then depends on the choice that must be made in expressing them in either the disturbances $(u_1, T_1^{(xy)})$ or $(u_2, T_2^{(xy)})$. Consequently, the physical meaning of such a decomposition of TAN is not clear. It thus seems that there is a discrepancy between our approach of the energy term TAN and that of Joseph and co-workers (Chen *et al.* 1990; Bai *et al.* 1992).

Table 3. Energy distribution for the long-wavelength instability of Yih (1967). As expected, the instability is due to viscosity stratification, which manifests itself through a viscosity-induced energy transfer TAN_v at the interface. The energy terms are for plane Couette flow in a channel with $\alpha = 0.1$, $R = 3.92 \times 10^{-3}$, $m = 0.05$, $r = 1$, $n = 2.5$, $S = 0$, $F = 0$, $\beta = 0$

KIN_1	KIN_2	DIS_1	DIS_2	REY_1	REY_2	TEN	HYD	TAN_v
0.99	0.01	-20318.95	-2729.69	0.00	-0.00	0.00	0.00	**23049.64**

readily be established for many papers in the literature, in the discussion below we will nevertheless discriminate between viscosity-induced and gravity-induced energy transfer. Some papers, however, report instabilities for which the energy transfer TAN cannot be simplified into either TAN_v or TAN_g. These papers are listed under the heading "viscosity-gravity-induced instability".

3.3.1. Viscosity-induced instability. A viscosity-induced stability finds its origin in a viscosity difference between the fluids, creating a jump in the slope U_j' of the basic-state velocity profile at the interface. When the interface is being deformed, continuity of total tangential velocity then forces a difference in magnitude between the velocity disturbances u_j at either side of the deformed interface (Smith 1990). This implies that a net amount of work is done by the primary flow at the interface (cf. [24]), which gives rise to an energy transfer TAN_v to the disturbed flow.

Pioneering theoretical work on the viscosity-induced type of instability was done by Yih (1967). Yih considered plane Couette–Poiseuille flow of two superposed layers of fluid of different viscosity and found instability for long waves, i.e. much longer than the layer thickness of either of the fluids. Because of the great relevance of this paper, table 3 gives an account of the energy contributions for Yih's long-wavelength instability in plane Couette flow. Obviously, the instability is driven by a viscosity-induced energy term TAN_v.

Instability due to viscosity stratification plays an important role in many papers dealing with the stability of both liquid–liquid as well as gas–liquid flow. In the context of liquid–liquid flow, the studies by Yih (1967), Li (1969). Akhtaruzzaman *et al.* (1978), Wang *et al.* (1978), Hooper and Boyd (1983), Hooper (1985, 1989), Renardy (1985, 1987a), Lister (1987), Than *et al.* (1987), Yiantsios and Higgins (1988), Anturkar *et al.* (1990), Weinstein and Kurz (1991), Miesen *et al.* (1992), Charru and Fabre (1994), Tilley *et al.* (1994) and Barthelet *et al.* (1995) can all be associated with viscosity-induced instability, where we note that papers that consider more than one type of instability shall be included in one of the other sections as well. The just mentioned papers report instabilities that are "long", "short" as well as "intermediate" in length for a certain number of different flow configurations, varying from two-layer Couette flow with each of the fluids occupying a semi-infinite domain to multilayer† flow down an inclined plane. Since these papers consider flow stability in a plane geometry, the results obtained therein can readily be reproduced by means of the numerical code outlined in section 2.1. Subsequent computation of the energy terms then shows the dominance of a viscosity-induced interface contribution TAN_v.

It should be noted that Joseph and co-workers have computed the various energy terms for *cylindrical* oil–water flow in tubes, yielding data that can be applied directly to experiments (Hu and Joseph 1989; Chen *et al.* 1990; Bai *et al.* 1992). Although our own numerical code was not designed to compute energy terms in a cylinder geometry, there is no doubt that the instabilities in the papers by Hickox (1971), Joseph *et al.* (1984), Renardy (1987b), Hu and Joseph (1989), Hu *et al.* (1990), Preziozi *et al.* (1989), Boomkamp and Miesen (1992) and Hu and Patankar (1995) are viscosity-induced in nature as well. This follows both from Joseph's computations and the fact that the stability problem in these papers is directly related to that of Miesen *et al.* (1992), who report viscosity-induced waves in *plane* oil–water flow.

In conclusion, we can state that viscosity stratification has been recognized for a long time as a possible cause of instability in liquid–liquid flow. It appears to be less well-recognized that viscosity-induced instability is very common in gas–liquid flow as well. Viscosity stratification accounts, for instance, for the generation of so-called capillary-gravity waves, both in the context

†Formally speaking, we should leave out of consideration papers dealing with more than two layers. This is because we have limited ourselves to two-layer flow. The papers by Li (1969), Akhtaruzzaman *et al.* (1978), Wang *et al.* (1978), Than *et al.* (1987), Anturkar *et al.* (1990) and Weinstein and Kurz (1991) nevertheless consider, among others, physical situations in which only viscosity stratification is a possible cause of instability.
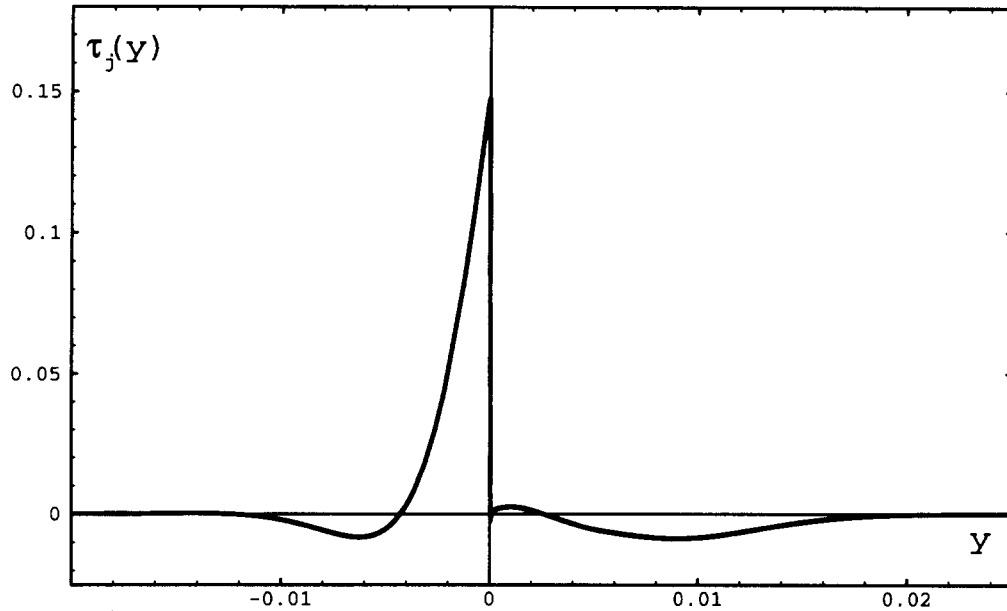
Figure 3. Characteristic Reynolds stress distribution $\tau_j(y)$ for capillary-gravity waves on deep water, using the parameters of table 4. The figure shows a small region in the air in which the Reynolds stress is positive, located directly above the interface. The instability is however induced by the viscosity difference between air and water (table 4) and not by this 'peak' in the Reynolds stress (Miles 1962). Note that in contrast to figure 2, the critical layer $y_c = 0.001$ now lies inside the viscous sublayer, which extends to $y = 0.0058$.

of deep water and thin films. For the case of unconfined flows, these waves have first been studied by Miles (1962), and after him by Valenzuela (1976), Kawai (1979) and Van Gastel et al. (1985), showing that the air velocity at which these waves are generated is significantly larger (u_* typically 0.2 m/s or more) than that for the Miles-instability (section 3.2). For these air velocities, the critical layer is located inside the viscous sublayer, which rules out the possibility of the mechanism discussed by Miles in his first two papers (1957, 1959a). In his fourth paper, Miles (1962) argues that the energy transfer to capillary-gravity waves is through the Reynolds stress in the air in the immediate neighbourhood of the interface. Despite the fact, however, that our computations show a small region in which the Reynolds stress is positive, located directly above the interface (figure 3), it is also clear that the energy transfer through the Reynolds stress in this region is far too small to account for the existence of capillary-gravity waves. Consequently, these waves are not generated by the mechanism proposed by Miles, but by the viscosity difference between air and water, which leads to a viscosity-induced energy transfer TAN_t at the interface. This is shown in table 4, using the linear-logarithmic profile [27] in the air and the exponential profile [28] in the water. The friction velocity u_* is chosen to be 0.21 m/s, which corresponds to a wind speed of roughly 4.5 m/s at two metres above the water. The wavelength is about 1.5 cm.

Viscosity-induced capillary-gravity waves can also arise if a (thin) film of liquid is sheared by a gas. In the 1960s, Cohen and Hanratty (1965) and Craik (1966) were the first to study this problem, both experimentally as well as theoretically. Cohen and Hanratty studied the conditions at which liquid films with a Reynolds number of typically one hundred become unstable, while Craik also

Table 4. Energy distribution for capillary-gravity waves. These waves are viscosity-induced in nature since they receive their energy from the interface contribution TAN_t. The energy terms are for wind over deep water, using a linear-logarithmic profile in the air [27] and an exponential profile in the water [28]. The parameter values used correspond to figure 5 in the paper by Van Gastel et al. (1985), which means $s = 5$, $n = \infty$, $b = 0.15$, $\alpha = 24$, $R = 1.98 \times 10^5$, $m = 0.018$, $r = 0.0012$, $S = 1.11 \times 10^{-4}$, $F = 5.39 \times 10^{-2}$, $\beta = 0$. This in turn corresponds to (in SI-units) $g = 9.8$, $\sigma = 0.0725$, $\rho_1 = 1.2$, $\rho_2 = 1000$, $\mu_1 = 1.8 \times 10^{-5}$, $\mu_2 = 0.001$, $d_2 = 0.06$, $u_* = 0.214$, $\tau = \rho_1 u_*^2 = 0.0550$, $U_0 = 0.098$, $U_i = 3.30$, $\lambda = 1.57 \times 10^{-2}$. The corresponding Reynolds stress distribution is shown in figure 3

KIN_1	KIN_2	DIS_1	DIS_2	REY_1	REY_2	TEN	HYD	TAN_t
0.12	0.88	−21.26	−0.53	−3.33	0.27	−0.71	−0.60	**27.16**

Table 5. Energy distribution for the gravity-induced instability. We see that the instability is driven by an energy transfer TAN_g at the interface, which is directly related to a density difference between the two fluids. The energy terms are for gravity-driven Poiseuille downflow in a vertical channel, using the parameter values $\alpha = 0.00525, R = 1.00, m = 1, r = 0.25,$
$n = 4, S = 3.17 \times 10^3, F = 0.93, \beta = \pi/2$

KIN_1	KIN_2	DIS_1	DIS_2	REY_1	REY_2	TEN	HYD	TAN_g
0.37	0.63	-7130309.87	-5235682.79	-0.04	-0.11	-1.23	0.00	**12365995.03**

studied smaller Reynolds numbers. The so-called "fast waves" found by Cohen and Hanratty are characterized by a wavelength that is typically 1–10 times the film thickness and a phase speed that is, in general, larger than the maximum liquid velocity. In contrast, the much longer waves reported by Craik for Reynolds numbers of the order one, have a phase speed that is nearly equal to the interfacial speed and are consequently called "slow-waves" (as shown by Jurman and McCready (1989b), the slow waves are "kinematic" in nature, while the fast waves can be considered "dynamic". This terminology derives from Lighthill and Whitham (1955)). Numerical computation of the energy terms reveals that both the fast as well as the slow waves are driven by a viscosity-induced interface contribution TAN_v. In the broad context of gas–liquid channel flow, we have checked that these waves play a role in papers by Blennerhassett (1980, 1987), Hanratty and co-workers (Hanratty 1983; Andritsos and Hanratty 1987; Andritsos 1992; Asali and Hanratty 1993), McCready and co-workers (Bruno and McCready 1989; Jurman et al. 1989; Jurman and McCready 1989; Peng et al. 1991; Jurman et al. 1992; Sangalli et al. 1992; Kuru et al. 1995) and Miesen and Boersma (1995), who all present theoretical and experimental work on the flow of air over low-viscosity liquids such as water or water–glycerine mixtures. Yih (1990) reports viscosity-induced instability in connection with a very viscous liquid film.

3.3.2. Gravity-induced instability. The gravity-induced instability originates at the interface and receives its energy from the work done by the component of gravity in the direction of the primary flow (in contrast to the Rayleigh–Taylor instability, which is driven by the component of gravity perpendicular to the interface). If the densities of the fluids differ and the angle of inclination β is nonzero, gravity affects the primary flow in the two phases in a different way, i.e. it leads to a jump in the curvature U_j'' of the basic-state velocity profile at the interface (Smith 1989). When the interface is being deformed, continuity of total tangential stress [22] then forces a difference in magnitude between the stress disturbances $T_j^{(xy)}$ at either side of the deformed interface (Smith 1990). In creating these stress disturbances a net amount of work is done by the primary flow at the interface, which leads to an energy transfer TAN_g to the disturbed flow ([26], table 5).

Probably the most well-known example of gravity-induced instability is the long-wavelength instability in film flow down an inclined plane, the film being bounded by a passive gas as its upper side. The stability of a single-phase falling film was first examined by Binnie (1957), Benjamin (1957) and Yih (1963). Binnie performed experiments on the onset of wave formation on a film of water flowing down a vertical wall, while Benjamin and Yih showed that the critical liquid Reynolds number beyond which instability occurs is proportional to the cotangent of the angle of inclination β. In deriving this result, Benjamin and Yih used a free surface approximation, i.e. they did not include the apparently small effect of the gas phase into their analysis, which is, of course, suggested by the fact that the shear stress τ at the gas–liquid interface is approximately zero. This approach has also been followed by Kelly et al. (1989) and Smith (1990, 1991), who give two different but in fact complementary explanations for the instability. Kelly et al. show that the energy transfer TAN_g to these waves is indeed through the disturbance shear stresses at the interface, while Smith uses a long-wavelength expansion to discuss the forces and flow patterns involved in creating instability. Additional contributions to the single-phase falling film problem have been made by Alekseenko et al. (1985), Floryan et al. (1987), Chin et al. (1986) and Giovine et al. (1991), among many others.

The flow of two or more fluids down an inclined plane was studied by Kao (1965a, 1965b, 1968), Akhtaruzzaman et al. (1978), Wang et al. (1978) and Weinstein and Kurz (1991). In such multilayer systems, density stratification can induce gravity-induced instability that originates either at the free surface ("surface mode") or at one of the liquid–liquid interfaces ("interfacial mode"). In addition, as was first shown by Renardy (1987b) and Smith (1989), gravity-induced instability can also apply

to gravity-driven Poiseuille flow in a pipe or a channel (table 5). Instabilities of this kind were reported by Chen et al. (1990) in the context of core–annular flow and by Hu and Patankar (1995) in the context of a freely rising thermal plume.

3.3.3. Viscosity-gravity-induced instability. It is important to keep in mind that the energy terms TAN_t and TAN_g, as discussed above, are only two manifestations of the *same* energy term TAN. Instabilities that are driven by this energy term can also manifest themselves in cases in which it is not possible to denote TAN as either viscosity-induced or gravity-induced ($m \neq 1, r \neq 1, \beta \neq 0$). We therefore note that the papers by Kao (1968), Hickox (1971), Akhtaruzzaman et al. (1978), Wang et al. (1978), Renardy (1987b), Chen et al. (1990), Weinstein and Kurz (1991), Bai et al. (1992), Tilley et al. (1994) and Hu and Patankar (1995) also report instabilities of the 'viscosity-gravity-induced' kind, in addition to viscosity-induced and/or gravity-induced instabilities.

3.4. Shear mode instability

As is well known, single-phase Poiseuille flow in a channel become unstable when the liquid flow rate exceeds a certain critical value. This "shear mode instability" is caused by a combination of the no-slip conditions at the boundaries and the viscous effects within the critical layer, which generates a destabilizing Reynolds stress (Drazin and Reid 1981). The unstable waves are known as Tollmien–Schlichting waves.

Table 6 shows the energy distribution for a two-phase analogue of these waves. The energy terms are for two-layer plane Couette flow, with the depth of the lower fluid bounded by a wall, while the depth of the upper fluid is unbounded (Hooper and Boyd 1987; Hooper 1989). The lower fluid is the less viscous and the instability is driven by the energy term REY_2. For the sake of clarity, we will briefly discuss the Reynolds stress distribution underlying this energy transfer, as depicted in figure 4. Due to the high value of the Reynolds number, the flow at either side of the interface can be considered inviscid, except for the regions that correspond to the viscous boundary layer at the wall, the viscous boundary layer at the interface and the critical layer. Since for zero profile curvature the presence of the critical layer can be ignored, this inviscid flow behaviour gives rise to a Reynolds stress distribution that is approximately constant throughout the bulk of either fluid (Lin 1955), its value being determined by the viscous effects at the wall and the interface. As shown asymptotically by Hooper and Boyd (1987), the viscous effects at the wall dominate over those at the interface, which means that the destabilizing energy transfer REY_2 in table 6 is primarily produced by the no-slip conditions at the solid boundary. With respect to the role of the interface in two-layer Couette flow, it is interesting to note that Hooper (1989) makes plausible that it has in fact taken over the role played by the critical layer in single-phase Poiseuille flow.

Unlike single-phase flow in a channel, which is only unstable in the case of Poiseuille flow, shear mode instability in liquid–liquid flow may also occur for Couette flow. The stability problem for these flow configurations has been studied theoretically by Renardy (1985), Hooper and Boyd (1987), Yiantsios and Higgins (1988), Hooper (1989) and Tilley et al. (1994), who all find shear mode instability if the (bulk average) liquid flow rate is sufficiently large. Experimental observations of unstable shear modes in two-layer channel flow have been reported by Charles and Lilleleht (1965), Kao and Park (1972) and Hame and Muller (1975). In a somewhat different context, i.e. for liquid–liquid flow through a cylindrical tube, Hu and Joseph (1989) argue that the emulsification of water into oil, as observed experimentally by Charles et al. (1961), is a direct consequence of shear mode instability.

In the preceding section, we have seen that film flow down an inclined plane is susceptible to a gravity-induced mode of instability. This instability originates at the interface and becomes

Table 6. Energy distribution for the shear mode instability, which is driven by the Reynolds stress REY_2 in the fluid with the lowest (kinematic) viscosity. The energy terms are for Couette flow of two superposed fluids with the depth of the lower fluid bounded by a wall, while the depth of the upper fluid is unbounded. The parameter values $\alpha = 0.076$, $R = 10^5$, $m = 5$, $r = 1$, $n = 40$ (simulating unbounded flow), $S = 0$, $F = 0$, $\beta = 0$ fall within the asymptotic regime studied by Hooper and Boyd (1987). The corresponding Reynolds stress distribution is shown in figure 4

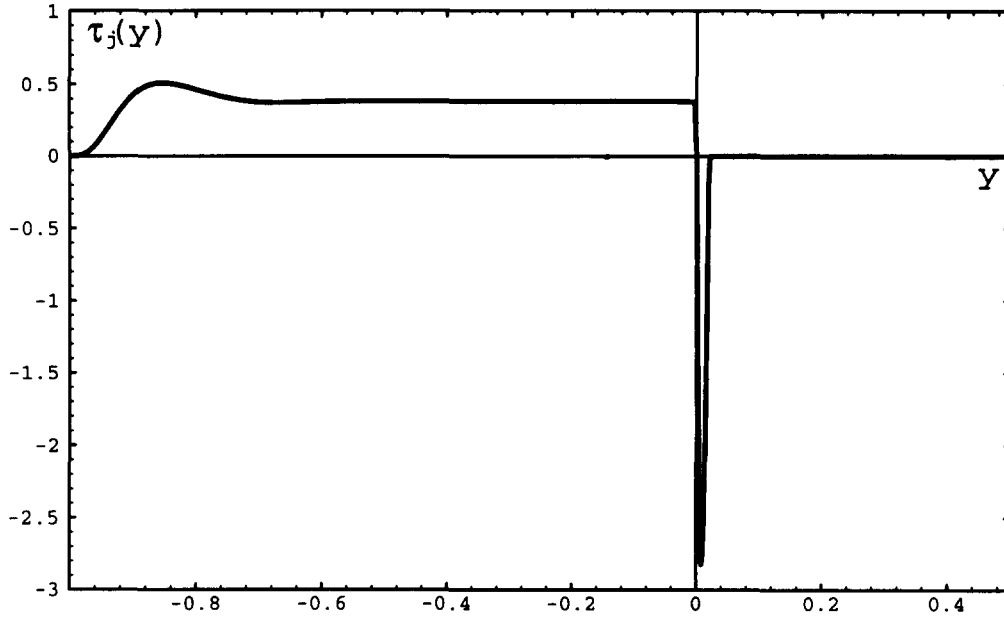| KIN_1	KIN_2	DIS_1	DIS_2	REY_1	REY_2	TEN	HYD	TAN_t
0.07	0.93	−0.00	−0.31	−0.00	**1.31**	0.00	0.00	0.00

Figure 4. Reynolds stress distribution $\tau_j(y)$ for the shear mode instability studied by Hooper and Boyd (1987) and Hooper (1989). The parameter values used are the same as those in table 6. Due to the disturbance vorticity generated at the solid boundary $y = -1$ and the presence of the interface, a positive Reynolds stress is induced in the lower fluid ($y < 0$), which accounts for a destabilizing energy transfer to the disturbed flow.

Table 7. Energy distribution for the internal mode, which arises if a thin liquid film is sheared by a gas, and the liquid Reynolds number exceeds a certain critical value. The instability is driven by *two* energy sources: the viscosity-induced interface contribution TAN_i and the Reynolds stress REY_2 in the liquid film. The energy terms are for a typical air–water system, using a linear-logarithmic profile in the air [27] and a linear profile in the water. The parameter values used correspond to figure 7 of the paper by Miesen and Boersma (1995), which means $s = 5$, $n = \infty$, $b = 3.5$, $\alpha = 0.91$, $R = 400$, $m = 0.018$, $r = 0.0012$, $S = 6.68 \times 10^{-2}$, $F = 1.84 \times 10^{-4}$, $\beta = 0$

KIN_1	KIN_2	DIS_1	DIS_2	REY_1	REY_2	TEN	HYD	TAN_i
0.39	0.61	−40.92	−0.89	−12.85	**2.97**	−0.07	−0.00	**52.76**

unstable for Reynolds numbers of the order of cot β. For liquid Reynolds numbers of $\mathcal{O}(10^3)$ or larger, however, the film is susceptible to shear mode instability as well. This mode of instability was identified by Lin (1967), who used, however, a wrong interfacial boundary condition in his analysis. The correct stability problem was addressed by De Bruin (1974), emphasizing that shear effects are the primary cause of instability when the angle of inclination becomes very small, the crossover occurring when $\beta \approx 0.5'$. Extensions of De Bruin's analysis were presented by Chin *et al.* (1986) and Floryan *et al.* (1987).

Finally, we note that Benjamin's "class-A instabilities", which are part of his threefold classification of instabilities of the flow of a liquid over a flexible solid (Benjamin 1960, 1963), also belong to the class of shear mode instability. The role of the Reynolds stress in the generation of these Tollmien–Schlichting waves† has been discussed by Benjamin (1960) himself as well as by Landahl (1962).

---

†In the context of gas–liquid flow, Miles (1962) has shown that capillary-gravity waves (section 3.3.1) result from the resonance between these Tollmien–Schlichting waves and the "free surface waves of the lower fluid". Since these Tollmien–Schlichting waves can naturally be associated with a Reynolds stress close to a rigid wall, it is possible that this feature has been a reason for Miles to relate the generation of capillary-gravity waves to a Reynolds stress directly above the gas–liquid interface. We have seen, however, that this statement is incorrect (table 4).

3.5. Internal mode

Until now, we have only encountered instabilities that are driven by a single source of energy. However, if a thin film of liquid is sheared by a gas, a mode of instability can arise that receives its energy from *two* sources: the viscosity-induced interface contribution TAN_t and the Reynolds stress in the liquid REY_2 (table 7: although $TAN_t \gg REY_2$, the Reynolds stress term is of importance because $KIN_1 + KIN_2 \equiv 1$). This mode is characterized by a wavelength that is typically one to ten times the film thickness and is only present for liquid Reynolds numbers that exceed a certain critical value, this value being typically 200 for air–water flow (Miesen and Boersma 1995). The name "internal" mode refers to the position of the critical layer, which is located in the bulk of the liquid film.

The dominance of the energy terms TAN_t and REY_2 suggests that the internal mode combines the physical mechanisms responsible for the viscosity-induced and the shear mode instability (section 3.3.1 and 3.4, respectively). The internal mode is nevertheless considered a separate mode because neither of these mechanisms is large enough to overcome the restoring effect of the dissipation in both fluids and the Reynolds stress in the gas, i.e. the two energy production terms are *both* essential. Surprisingly, our computations reveal that in a plane geometry only the parameters corresponding to the thin film problem give rise to a mode of instability that is driven by more than one source of energy.

Compared to the extensive literature on the other classes of instability, little attention has been paid to the internal mode. As far as we know, the internal mode has been studied by Miles (1960), Smith and Davis (1982) and Miesen and Boersma (1995) only. This scarcity of literature can be explained in two ways. In the first place, experimental observation of the internal mode is extremely difficult, because for conditions at which this mode becomes unstable, the viscosity-induced capillary-gravity waves as described in section 3.3.1 are unstable already. Secondly, as stated before, only the parameters corresponding to the thin film problem give rise to an internal mode, which implies that the physical meaning of this mode is limited to a small region in parameter space.

In describing the internal mode Miles (1960) and Smith and Davis (1982) use a "free surface approximation", i.e. they assume that the dynamic influence of the gas stress *variations* on the liquid interface is negligible. This approximation requires the density and the dynamic viscosity of the liquid to be much larger than those of the gas, while its kinematic viscosity should be much smaller (Miles 1960). Although for instance an air–water system seems to meet these requirements, Miesen and Boersma (1995) have recently shown that the error that is introduced by this approximation is, in general, significant. In energetic terms, this can be illustrated as follows. By definition, the free surface approximation leaves out of consideration the energy terms TAN_t, KIN_1, DIS_1 and REY_1. According to table 7, the net amount of energy that is thus neglected is approximately equal to 1.4, which is significant if compared to the rate of change of the disturbance kinetic energy KIN_2 in the film. This outcome illustrates Miesen and Boersma's conclusion that the stress variations in the gas *do* have an appreciable effect on the stability of the film.

4. CLOSING REMARKS

In this paper we have presented an overview of a major part of the extensive literature on the stability of parallel two-phase flow. By analyzing systematically the energy transfer between the primary flow and the disturbed flow, we were able to indicate which papers in the field of hydrodynamic stability in fact study the same *type* of instability. As such, this literature can be classified into five groups, based on the five different mechanisms by which energy transfer can take place. These mechanisms find their origin in one of the following properties of the flow system: density stratification and orientation (sections 3.1 and 3.3), velocity profile curvature (section 3.2), viscosity stratification (section 3.3), shear effects (section 3.4) or a combination of viscosity stratification and shear effects (section 3.5). The fact that we consider a *plane* flow configuration (figure 1) rules out the possibility of capillary instability, so that instability driven by the interfacial tension energy term TEN was not encountered.

We note that it is in principle possible to make a subdivision of each of the five classes of instability by looking not only at the energy production terms in the energy equation [11], but at

the *consumption* terms as well. In that case, each subclass can naturally be associated with a characteristic energy distribution over *all* the energy terms. However, because this procedure does not really add to the transparency of our scheme, we have refrained from actually making such a refinement.

The scheme also allows for a somewhat different kind of refinement.† Since we have at our disposal the numerical solution of the stability problem, it is possible to further decompose the energy transfer TAN at the interface into two separate terms, $TAN_1 = -u_1 T_1^{(\gamma)}$ and $TAN_2 = u_2 T_2^{(\gamma)}$. These terms represent the rate at which the tangential velocity and stress disturbances do work at *either* side of the interface, thus showing to what extent either of the two phases is involved in the *net* energy transfer TAN, as defined in [17]. Implementation of this modification into our numerical code shows that viscosity-induced instability (section 3.3.1) is mainly associated with the velocity disturbances in the less viscous fluid. This is in line with intuition, since in this fluid the slope of the basic-state velocity profile is the largest, which accounts for relatively large velocity disturbances at that side of the (deformed) interface. Similarly, we found that the destabilizing energy transfer TAN_g in the case of gravity-induced instability (section 3.3.2) is mainly caused by the stress disturbances in the fluid with the highest density, a fluid property that leads to relatively large stress disturbance at that side of the (deformed) interface. Exceptions to these observations were not found, which means that even though the internal mode (section 3.5) has historically been associated with the dynamics of the liquid film, the destabilizing energy term TAN_i is also for this mode primarily caused by the gas dynamics, i.e. by the less viscous fluid.

Although the added value of our classification scheme lies especially in its transparency and completeness, we have made a few interesting corrections to the existing literature as well. It was for instance found (section 3.3.1) that the generation of capillary-gravity waves cannot be explained by the presence of a positive Reynolds stress directly above the gas–liquid interface, as argued by Miles (1962); these waves must be associated with the viscosity jump at the interface. Furthermore, we have seen that the internal mode (section 3.5) is actually driven by two sources of energy, while this mode has traditionally been associated with shear effects only (Miles 1960; Smith and Davis 1982). Another interesting feature of our fivefold classification scheme, which has not been discussed before, is that the classical Kelvin–Helmholtz instability is lacking. This instability corresponds to the third possible kind of instability in Benjamin's scheme of instabilities of the flow of a liquid over a flexible solid (Benjamin 1963). As is well known, the original Kelvin–Helmholtz model refers to the flow of two inviscid fluids in relative motion, each fluid having constant velocity (Drazin and Reid 1981). For a velocity difference surpassing some critical value, the destabilizing effect of suction dominates the stabilizing effect of gravity and interfacial tension, thus causing instability. In energetic terms, this instability is driven by the Reynolds stress in the vortex sheet at the interface. This can readily be seen from the energy equation [11], realizing that the dissipation terms DIS_j and the interface contribution TAN vanish for inviscid flow, and that work is done against the gravity and interfacial tension forces. This implies that only the Reynolds stress in the vortex sheet is a possible source of energy.

In his third paper (1959b), Miles has modified the original Kelvin–Helmholtz model to allow for variation in the fluid velocities with distance from the interface. He argues that the instability is important for a viscous liquid sheared by air, referring to an experiment by Francis for air blowing over oil (Francis 1954). Using the same physical parameters as Miles (section 4), however, our numerical computations only retrieve a mode of instability that is viscosity-induced in nature (section 3.3.1), i.e. this instability is not of the Kelvin–Helmholtz type. Furthermore, computations for other air–liquid combinations have not provided any evidence of the Kelvin–Helmholtz instability. This suggests that including viscous effects, however small, into the stability problem (section 2.1), rules out the possibility of the essentially inviscid Kelvin–Helmholtz instability. This observation seems to be supported by the recent work of Kuru *et al.* (1995), who present numerical computations of the gas–liquid stability problem for a wide range of liquid viscosities, using the exact Orr–Sommerfeld differential formulation. Subsequent comparison of these results with

---

†The authors are indebted to F. Charru and M. K. Smith for making this suggestion during the AMS-IMS-SIAM summer research conference in Seattle, U.S.A., July 1995.

simplified models like Kelvin–Helmholtz, integral momentum and long waves expansion approaches makes clear that such models are not reliable in predicting the onset of instability.

REFERENCES

Akhtaruzzaman, A. F. M., Wang, C. K. and Lin, S. P. (1978) Wave motion in multilayered liquid films. *J. Appl. Mech.* **45**, 25–31.

Alekseenko, S. V., Nakoryakov, V. E. and Pokusaev, B. G. (1985) Wave formation on vertical falling films. *Int. J. Multiphase Flow* **11**, 607–627.

Andritsos, N. and Hanratty, T. J. (1987) Interfacial instabilities for horizontal gas–liquid flows in pipelines. *Int. J. Multiphase Flow* **13**, 583–603.

Andritsos, N. (1992) Statistical analysis of waves in horizontal stratified gas–liquid flow. *Int. J. Multiphase Flow* **18**, 465–473.

Anturkar, N. R., Papanastasiou, T. C. and Wilkes, J. O. (1990) Linear stability analysis of multilayer plane Poiseuille flow. *Phys. Fluids A* **2**, 530–541.

Asali, J. C. and Hanratty, T. J. (1993) Ripples generated on a liquid film at high gas velocities. *Int. J. Multiphase Flow* **19**, 229–243.

Bai, R., Chen, K. and Joseph, D. D. (1992) Lubricated pipelining: stability of core–annular flow. Part 5. Experiments and comparison with theory. *J. Fluid Mech.* **240**, 97–132.

Barthelet, P., Charru, F. and Fabre, J. (1995) Experimental study of interfacial long waves in a two-layer shear flow. *J. Fluid Mech.* **303**, 23–53.

Belcher, S. E. and Hunt, J. C. R. (1993) Turbulent shear flow over slowly moving waves. *J. Fluid Mech.* **251**, 109–148.

Benjamin, T. B. (1957) Wave formation in laminar flow down an inclined plane. *J. Fluid Mech.* **2**, 554–574.

Benjamin, T. B. (1959) Shearing flow over a wavy boundary. *J. Fluid Mech.* **6**, 161–205.

Benjamin, T. B. (1960) Effects of a flexible boundary on hydrodynamic stability. *J. Fluid Mech.* **9**, 513–532.

Benjamin, T. B. (1963) The threefold classification of unstable disturbances in flexible surfaces bounding inviscid flows. *J. Fluid Mech* **16**, 436–450.

Binnie, A. M. (1957) Experiments on the onset of wave formation on a film of water down a vertical plane. *J. Fluid Mech.* **2**, 551–553.

Blennerhassett, P. J. (1980) On the generation of waves by wind. *Phil. Trans. Roy. Soc. A* **298**, 451–494.

Blennerhassett, P. J. and Smith, F. R. (1987) Short-scale waves on wind-driven water. *Proc. Roy. Soc. Lond. A* **410**, 1–17.

Boomkamp, P. A. M. and Miesen, R. H. M. (1993) Nonaxisymmetric waves in core–annular flow with a small viscosity ratio. *Phys. Fluids A* **4**, 1627–1636.

Boomkamp, P. A. M. and Miesen, R. H. M. (1996) Physical characteristics of instabilities in parallel two-phase flow. In *Advances in Multi-fluid flow, Proc. AMS-IMS-SIAM Conf. Analysis of Multi-fluid Flows and Interfacial Instabilities*, ed. Y. Renardy. SIAM, Philadelphia.

Boomkamp, P. A. M., Boersma, B. J., Miesen, R. H. M. and Beijnon, G. (1997) A Chebyshev collocation method for solving two-phase flow stability problems. *J. Comput. Phys.* (to appear).

Bruin, G. J. de (1974) Stability of a layer of liquid flowing down an inclined plane. *J. Eng. Math.* **8**, 259–270.

Bruno, K. and McCready, M. J. (1989) Processes which control the interfacial wave spectrum in separated gas–liquid flows. *Int. J. Multiphase Flow* **15**, 531–552.

Caponi, E. A., Caponi, M. Z., Saffman, P. G. and Yuen, H. C. (1992) A simple model for the effect of water shear on the generation of waves by wind. *Proc. Roy. Soc. Lond. A* **438**, 95–101.

Chandrasekhar, S. (1961) *Hydrodynamic and Hydromagnetic Stability*. Dover, New York.

Charles, M. E., Govier, G. W. and Hodgson, G. W. (1961) The horizontal pipeline flow of equal density oil–water mixtures. *Can. J. Chem. Engng* **39**, 17–36.

Charles, M. E. and Lilleleht, L. U. (1965) An experimental investigation of stability and interfacial waves in co-current flow of two liquids. *J. Fluid Mech.* **22**, 217–224.

Charru, F. and Fabre, J. (1994) Long waves at the interface between two viscous fluids. *Phys. Fluids* **6**, 1223–1235.

Chen, K., Bai, R. and Joseph, D. D. (1990) Lubricated pipelining. Part 3. Stability of core–annular flow in vertical pipes. *J. Fluid Mech.* **214**, 251–286.

Chen, K. and Joseph, D. D. (1991) Lubricated pipelining: stability of core–annular flow. Part 4. Ginzburg–Landau equations. *J. Fluid Mech.* **227**, 587–615.

Chin, R. W., Abernathy, F. H. and Berschy, J. R. (1986) Gravity and shear wave instability of free surface flows. Part 1. Numerical calculations. *J. Fluid Mech.* **168**, 501–513.

Cohen, L. S. and Hanratty, T. J. (1965) Generation of waves in the concurrent flow of air and a liquid. *AIChEJ.* **11**, 138–144.

Conte, S. D. and Miles, J. W. (1959) On the numerical integration of the Orr–Sommerfeld equation. *J. Soc. Indust. Appl. Meth.* **7**, 361–366.

Craik, A. D. D. (1966) Wind-generated waves in thin liquid films. *J. Fluid Mech.* **26**, 369–392.

Craik, A. D. D. (1976) Rayleigh–Taylor instability of thin viscous layers. *Phys. Fluids* **19**, 479–480.

Dijkstra, H. A. (1992) The coupling of interfacial instabilities and the stabilization of two-layer annular flows. *Phys. Fluid A* **4**, 1915–1928.

Drazin, P. G. and Reid, W. H. (1981) *Hydrodynamic Stability*. Cambridge University Press, Cambridge.

Duin, C. A. van and Janssen, P. A. E. M. (1992) An analytical model of the generation of surface gravity waves of turbulent air flow. *J. Fluid Mech.* **236**, 197–215.

Floryan, J. M., Davis, S. H. and Kelly, R. E. (1987) Instabilities of a liquid film flowing down a slightly inclined plane. *Phys. Fluids* **30**, 983–989.

Francis, J. R. D. (1954) Wave motion and the aerodynamic drag on a free oil surface. *Phil. Mag.* **45**, 695–702.

Gastel, K. van, Janssen, P. A. E. M. and Komen, G. J. (1985) On phase velocity and growth rate of wind-induced gravity-capillary waves. *J. Fluid Mech.* **161**, 199–216.

Giovine, P., Minervini, A. and Andreussi, P. (1991) Stability of liquid flow down an inclined tube. *Int. J. Multiphase Flow* **17**, 485–496.

Hall-Taylor, N. S. and Hewitt, G. F. (1962) The motion and frequency of disturbance waves in annular two-phase flow of air–water mixtures. AERE-R 3955, Harwell, England.

Hame, W. and Muller, U. (1975) On the stability of a plane two-layer Poiseuille flow. *Acta Mech.* **23**, 75–89.

Hanratty, T. J. (1983) Interfacial instabilities caused by air flow. In *Waves on Fluid Interfaces*, ed. R. E. Meyer. Academic Press, New York.

Hickox, C. E. (1971) Instability due to viscosity and density stratification in axisymmetric pipe flow. *Phys. Fluids* **14**, 251–262.

Hinch, E. (1984) A note on the mechanism of the instability at the interface between two shearing fluids. *J. Fluid Mech.* **144**, 463–465.

Hooper, A. P. and Boyd, W. G. C. (1983) Shear-flow instability at the interface between two viscous fluids. *J. Fluid Mech.* **128**, 507–528.

Hooper, A. P. (1985) Long-wave instability at the interface between two viscous fluids: thin layer effects. *Phys. Fluids* **28**, 1613–1618.

Hooper, A. P. and Boyd, W. G. C. (1987) Shear-flow instability due to a wall and a viscosity discontinuity at the interface. *J. Fluid Mech.* **179**, 201–225.

Hooper, A. P. (1989) The stability of two superposed viscous fluids in a channel. *Phys. Fluids A* **1**, 1133–1142.

Hu, H. H. and Joseph, D. D. (1989) Lubricated pipelining: stability of core–annular flow. Part 2. *J. Fluid Mech.* **205**, 359–396.

Hu, H. H., Lundgren, T. S. and Joseph, D. D. (1990) Stability of core–annular flow with a small viscosity ratio. *Phys. Fluids A* **2**, 1945–1954.

Hu, H. H. and Patankar, N. (1995) Nonaxisymmetric instability of core–annular flow. *J. Fluid Mech.* **290**, 213–224.

Jeffreys, H. (1925) On the formation of water waves by wind. *Proc. Roy. Soc. Lond. A* **107**, 189–206.

Joseph, D. D., Renardy, M. and Renardy, Y. Y. (1984) Instability of the flow of two immiscible liquids with different viscosities in a pipe. *J. Fluid Mech.* **141**, 309–317.

Joseph, D. D. and Renardy, Y. Y. (1993) *Fundamentals of Two-fluid Dynamics, Part II: Lubricated Transport, Drops and Miscible Fluids*. Springer, New York.

Jurman, L. A., Bruno, K. and McCready, M. J. (1989) Periodic and solitary waves on thin, horizontal, gas-sheared liquid films. *Int. J. Multiphase Flow* **15**, 371–384.

Jurman, L. A. and McCready, M. J. (1989) Study of waves on thin liquid films sheared by turbulent gas flows. *Phys. Fluids A* **1**, 522–536.

Jurman, L. A., Deutch, S. E. and McCready, M. J. (1992) Interfacial mode interactions in horizontal gas–liquid flow. *J. Fluid Mech.* **238**, 187–219.

Kao, T. W. (1956a) Stability of two-layer viscous stratified flow down an inclined plane. *Phys. Fluids* **8**, 812–820.

Kao, T. W. (1965b) Role of the interface in the stability of stratified flow down an inclined plane. *Phys. Fluids* **8**, 2190–2194.

Kao, T. W. (1968) Role of viscosity stratification in the stability of two-layer flow down an incline. *J. Fluid Mech.* **33**, 561–572.

Kao, T. W. and Park, C. (1972) Experimental investigation of the stability of channel flow. Part 2. Two-layered co-current flow in a rectangular channel. *J. Fluid Mech.* **52**, 401–423.

Kawai, S. (1979) Generation of initial wavelets by instability of a coupled shear flow and their evolution to wind waves. *J. Fluid Mech.* **93**, 661–703.

Kelly, R. E., Goussis, D. A., Lin, S. P. and Hsu, F. K. (1989) The mechanism of surface wave instability in film flow down an inclined plane. *Phys. Fluids A* **1**, 819–828.

Kumaran, V. (1995) Stability of the flow of a fluid through a flexible tube at high Reynolds number. *J. Fluid Mech.* **302**, 117–139.

Kuru, W. C., Sangalli, M., Uphold, D. D. and McCready, M. J. (1995) Linear stability of stratified channel flow. *Int. J. Multiphase Flow* **21**, 733–753.

Landahl, M. T. (1962) On the stability of a laminar incompressible boundary layer over a flexible surface. *J. Fluid Mech.* **13**, 609–632.

Lewis, D. J. (1950) The instability of liquid surfaces when accelerated in a direction perpendicular to their planes (II). *Proc. Roy. Soc. A* **117**, 81–96.

Li, C. H. (1969) The instability of three-layer viscous stratified flow. *Phys. Fluids* **12**, 2473–2481.

Lighthill, M. J. and Williams, G. B. (1955). On kinematic waves: I. Flood movement in long rivers; II. Theory of traffic flow on long crowded roads. *Proc. Roy. Soc. A* **229**, 281–345.

Lighthill, M. J. (1962) Physical interpretation of the mathematical theory of wave generation by wind. *J. Fluid Mech.* **14**, 385–398.

Lin, C. C. (1955) *The Theory of Hydrodynamic Stability*. Cambridge University Press, Cambridge.

Lin, S. P. (1967) Instability of a liquid film flowing down an inclined plane. *Phys. Fluids* **10**, 308–313.

Lister, J. R. (1987) Long-wavelength instability of a line plume. *J. Fluid Mech.* **175**, 413–428.

Long, R. B. (1980) A parametric model for the vertical structure of the induced atmospheric pressure field above a spectrum of surface gravity waves. *J. Fluid Mech.* **99**, 163–183.

Miesen, R. H. M., Beijnon, G., Duijvestijn, P. E. M., Oliemans, R. V. A. and Verheggen, T. M. M. (1992) Interfacial waves in core–annular flow. *J. Fluid Mech.* **238**, 97–117.

Miesen, R. H. M. (1993) Hydrodynamic stability of parallel flows of fluids with different viscosities. AMER.93.003, Koninklijke/Shell-Laboratorium, Amsterdam.

Miesen, R. H. M. and Boersma, B. J. (1995) Hydrodynamic stability of a sheared liquid film. *J. Fluid Mech.* **301**, 175–202.

Miles, J. W. (1957) On the generation of surface waves by shear flows. *J. Fluid Mech.* **3**, 185–204.

Miles, J. W. (1959a) On the generation of surface waves by shear flows. Part 2. *J. Fluid Mech.* **6**, 568–582.

Miles, J. W. (1958b) On the generation of surface waves by shear flows, Part 3: Kelvin–Helmholtz instability. *J. Fluid Mech.* **6**, 583–598.

Miles, J. W. (1959c) On the generation of surface waves by turbulent shear flows. *J. Fluid Mech.* **7**, 469–478.

Miles, J. W. (1960) The hydrodynamic stability of a thin film of liquid in uniform shearing motion. *J. Fluid Mech.* **8**, 593–610.

Miles, J. W. (1962) On the generation of surface waves by shear flows, Part 4. *J. Fluid Mech.* **13**, 433–448.

Miles, J. W. (1967) On the generation of surface waves by shear flows, Part 5. *J. Fluid Mech.* **30**, 163–175.

Miles, J. W. (1993) Surface-wave generation revisited. *J. Fluid Mech.* **256**, 427–441.

Molar, C. B. and Stewart, G. W. (1973) An algorithm for generalized matrix eigenvalue problems. *SIAM J. Num. Anal.* **10**, 241–256.

Morland, L. C. and Saffman, P. G. (1993) Effect of wind profile on the instability of wind blowing over water. *J. Fluid Mech.* **252**, 383–398.

The NAG Fortran Library Manual—Mark 13, ISBN 1-85206-040-9, NAG Ltd, Oxford.

Peng, C. A., Jurman, L. A. and McCready, M. J. (1991) Formation of solitary waves on gas-sheared liquid layers. *Int. J. Multiphase Flow* **17**, 767–782.

Plesset, M. S. and Whipple, C. G. (1974) Viscous effects in Rayleigh–Taylor instability. *Phys. Fluids* **17**, 1–7.

Preziosi, L., Chen, K. and Joseph, D. D. (1989) Lubricated pipelining: stability of core–annular flow. *J. Fluid Mech.* **201**, 323–356.

Prosperetti, A. (1981) Motion of two superposed viscous fluids. *Phys. Fluids* **24**, 1217–1223.

Rayleigh, Lord (1983) Investigation of the character of the equilibrium of an incompressible heavy fluid of variable density. *Proc. London Math. Soc.* **14**, 170–177. Also *Scientific Papers* (Vol. II) (1900) Cambridge University Press, pp. 200–207.

Renardy, Y. (1985) Instability at the interface between two shearing fluids in a channel. *Phys. Fluids* **28**, 3441–3443.

Renardy, Y. (1987a) The thin-layer effect and interfacial stability in a two-layer Couette flow with similar liquids. *Phys. Fluids* **30**, 1627–1637.

Renardy, Y. (1987b) Viscosity and density stratification in vertical Poiseuille flow. *Phys. Fluids* **30**, 1638–1648.

Sangalli, M., Prokopiou, Th., McCready, M. J. and Chang, H. C. (1992) Observed transitions in two-phase stratified gas–liquid flow. *Chem. Engng Sci.* **47**, 3289–3296.

Schlichting, H. (1955) *Boundary-layer Theory*. McGraw-Hill, New York.

Smith, M. K. and Davis, S. H. (1982) The instability of sheared liquid layers. *J. Fluid Mech.* **121**, 187–206.

Smith, M. K. (1989) The axisymmetric long-wave instability of a concentric two-phase pipe flow. *Phys. Fluids A* **1**, 494–506.

Smith, M. K. (1990) The mechanism for the long-wave instability in thin liquid films. *J. Fluid Mech.* **217**, 469–485.

Smith, M. K. (1985) The role of the inviscid model for the long-wave instability of an inclined liquid layer. *Phys. Fluids A* **3**, 2813–2815.

Synder, R. L., Dobson, F. W., Elliot, J. A. and Long, R. B. (1981) Array measurements of atmospheric pressure fluctuations above surface gravity waves. *J. Fluid Mech.* **102**, 1–59.

Squire, H. B. (1933) On the stability for three-dimensional disturbances of viscous fluid flow between parallel walls. *Proc. Roy. Soc. A* **142**, 621.

Taylor, G. I. (1950) The stability of liquid surfaces when accelerated in a direction perpendicular to their planes (I). *Proc. Roy. Soc.* **201**, 192–196.

Than, P. T., Rosso, F. and Joseph, D. D. (1987) Instability of Poiseuille flow of two immiscible liquids with different viscosities in a channel. *Int. J. Engng Sci.* **25**, 189–204.

Tilley, B. S., Davis S. H. and Bankoff, S. G. (1994) Linear stability theory of two-layer fluid flow in an inclined channel. *Phys. Fluids* **6**, 3906–3922.

Valenzuela, G. R. (1976) The growth of gravity-capillary waves in a coupled shear flow. *J. Fluid Mech.* **76**, 229–250.

Wang, C. K., Seaborg, J. J. and Lin, S. P. (1978) Instability of multi-layered liquid films. *Phys. Fluids* **21**, 1669–1673.

Weinstein, S. J. and Kurz, M. R. (1991) Long-wavelength instabilities in three-layer flow down an incline. *Phys. Fluids A* **3**, 2680–2687.

Whitehead, J. A. and Luther, D. S. (1975) Dynamics of laboratory diapir and plume models. *J. Geophys. Res.* **80,** 705–717.

Whitehead, J. A. (1988) Fluid models of geological hotspots. *Ann. Rev. Fluid Mech.* **20,** 61–87.

Yiantsios, S. G. and Higgins, B. G. (1988) Linear stability of plane Poiseuille flow of two superposed fluids. *Phys. Fluids* **31,** 3225–3238 and Erratum *Phys. Fluids A* **1,** 897.

Yiantsios, S. G. and Higgins, B. G. (1988) Rayleigh–Taylor instability in thin viscous films. *Phys. Fluids A* **1,** 1484–1501.

Yih, C.-S. (1955) Stability of two-dimensional parallel flows for three-dimensional disturbances. *Quart. Appl. Math.* **12,** 434.

Yih, C.-S. (1963) Stability of liquid flow down an inclined plane. *Phys. Fluids* **6,** 321–334.

Yih, C.-S. (1967) Instability due to viscosity stratification. *J. Fluid Mech.* **27,** 337–352.

Yih, C.-S. (1990) Wave formation on a liquid layer for de-icing airplane wings. *J. Fluid Mech.* **212,** 41–53.